Electronic Supplementary Material (ESI) for RSC Advances

Supporting Information

A NOVEL SYNTHETIC STRATEGY FOR BIOINSPIRED FUNCTIONALLY GRADED NANOCOMPOSITES EMPLOYING MAGNETIC FIELD GRADIENTS

COMPUTATION OF THE MAGNETIC FIELDS AND RELATED FORCES

The magnetic flux densities outside the block magnets were determined by the following equations[1]

$$\overline{B}_x(x,y,z)=\frac{\mu_0\overline{M}_s}{4\pi}\sum_{k=1}^{2}\sum_{m=1}^{2}(-1)^{k+m}\ln\left[\frac{(y-y_1)+\left[(x-x_m)^2+(y-y_1)^2+(z-z_k)^2\right]^{1/2}}{(y-y_2)+\left[(x-x_m)^2+(y-y_2)^2+(z-z_k)^2\right]^{1/2}}\right] \quad \text{(S1)}$$

$$\overline{B}_y(x,y,z)=\frac{\mu_0\overline{M}_s}{4\pi}\sum_{k=1}^{2}\sum_{m=1}^{2}(-1)^{k+m}\ln\left[\frac{(x-x_1)+\left[(x-x_1)^2+(y-y_m)^2+(z-z_k)^2\right]^{1/2}}{(x-x_2)+\left[(x-x_2)^2+(y-y_m)^2+(z-z_k)^2\right]^{1/2}}\right] \quad \text{(S2)}$$

$$\overline{B}_z(x,y,z)=\frac{\mu_0\overline{M}_s}{4\pi}\sum_{k=1}^{2}\sum_{m=1}^{2}\sum_{n=1}^{2}(-1)^{k+m+n}ArcTan\left[\frac{(x-x_n)(y-y_m)}{(z-z_k)\left[(x-x_n)^2+(y-y_m)^2+(z-z_k)^2\right]^{-1/2}}\right] \quad \text{(S3)}$$

where B_x, B_y and B_z are the magnetic fields in the x, y and z directions, respectively, μ_0 is the vacuum permeability, Ms is the saturation magnetization of the magnet and (x_1, x_2), (y_1, y_2) and (z_1, z_2) are the positions of the edges of the magnet, which is magnetized along the z-axis. The magnetic flux densities (verified by a Hall probe magnetometer), magnetic field gradients and magnetic forces were evaluated setting $M_s = 10.5 \cdot 10^5$ A/m and x_1 = -0.02, x_2 = 0.02, y_1 = -0.02, y_2 = 0.02, z_1 = -0.02, z_2 = 0. This was done in order to ascertain which magnets arrangements give rise to the highest z component of $\overline{F}_m$, which is the driving force for the gradient formation along the z-axis. For the single magnet case, the z component of $\overline{F}_m$ follows the behavior of the gradient of the magnetic induction along z and goes through a maximum positioned 2 mm away from the surface of the magnet (Figure S1). An increment in magnetic force can be achieved when two magnets in repulsion configuration are employed because in this case the gain in the gradient of the magnetic flux density

dB_z (Figure S1) can overcome the loss in the nanoparticle magnetic moment m (due to the decrease in magnetic flux density), resulting in an higher magnetic force compared to the single magnet case. On the contrary, when two magnets in attraction configuration are employed the increment in the particle magnetic moment (due to the increment in magnetic induction intensity) can only partially compensate the loss in the modulus of the induction gradient, and the z component of the magnetic force will tend at best, at quite large distances d between the magnets, to that generated by a single magnet.

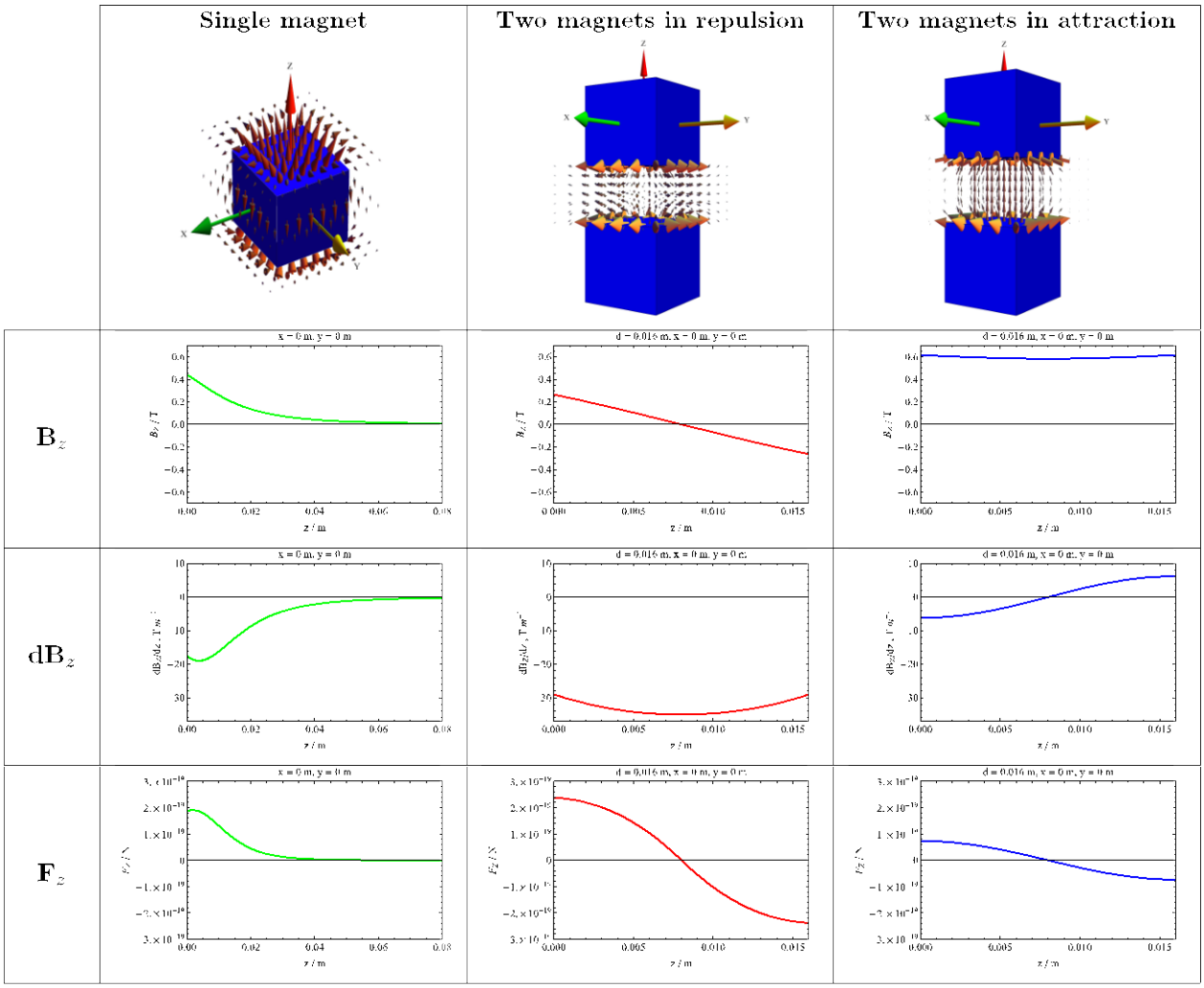

Figure S1. Table comparing the magnetic induction B, its gradient dB with respect to the z-direction and the magnetic force F exerted on a single Fe_3O_4 nanoparticle for the single magnet case and the cases of two magnets in repulsion and attraction configurations. All the quantities are considered along the direction over which the gradient is wanted (z-direction).

PREPARATION OF THE NANOPARTICULATE THIN FILMS

Considering the case of the two magnets in repulsion configuration, we can see (Figure S2-a) that a much higher z-component of the magnetic force is generated towards the edges of the magnet, which spans the region from x=-0.02 m to x=0.02 m. In that same region, however, even the x-component (and for symmetry also the y-component) of F_m shows a noticeable increase (Figure S2-b), eventually overcoming the force acting in the z-direction upon reaching the edges of the magnet and making the formation of the gradient along the z-axis less controllable.

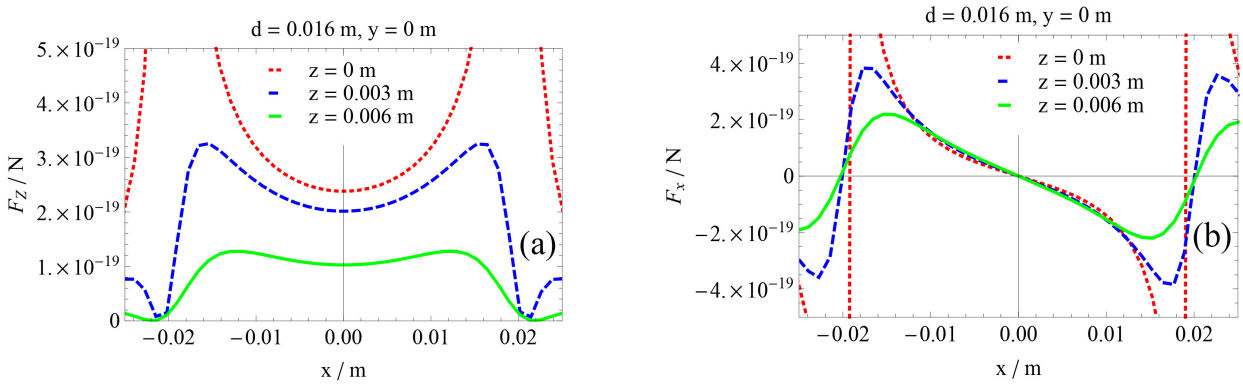

Figure S2. Plot of *z*- (a) and *x*- (b) components of the magnetic force F_m acting on a Fe_3O_4 nanoparticle placed at different distances *z* from the magnet for the case of two magnets in repulsion configuration. The two magnets are placed at a distance d = 1.6 cm from each other.

It was therefore important to define a central area in which the z-component of the magnetic force was predominant over the x- and y- ones. In particular, the sample was confined on a central area (1 cm x 1 cm) over the bottom magnet (Figure S3) on which, point-by-point, the magnitude of the x-component of the magnetic force was always smaller than half of the magnitude of the z-component. By doing so, the gradient formation along the z-direction was not hindered by the action of the x- and y- components of the magnetic force.

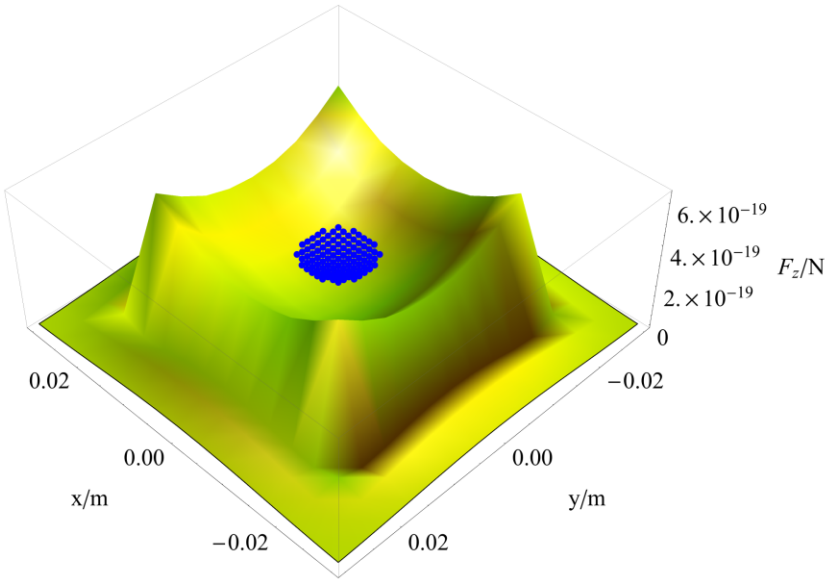

Figure S3. 3D- plot of z-component of the magnetic force F_m exerted on a Fe_3O_4 nanoparticle placed at z=0 between two magnets at a distance d=1.6 cm. The blue points define the area over which $F_x \leq 0.5\ F_z$.

IR ANALYSIS OF Fe_3O_4@SILICA AND Fe_3O_4@SILICA-MPS NANOPARTICLES

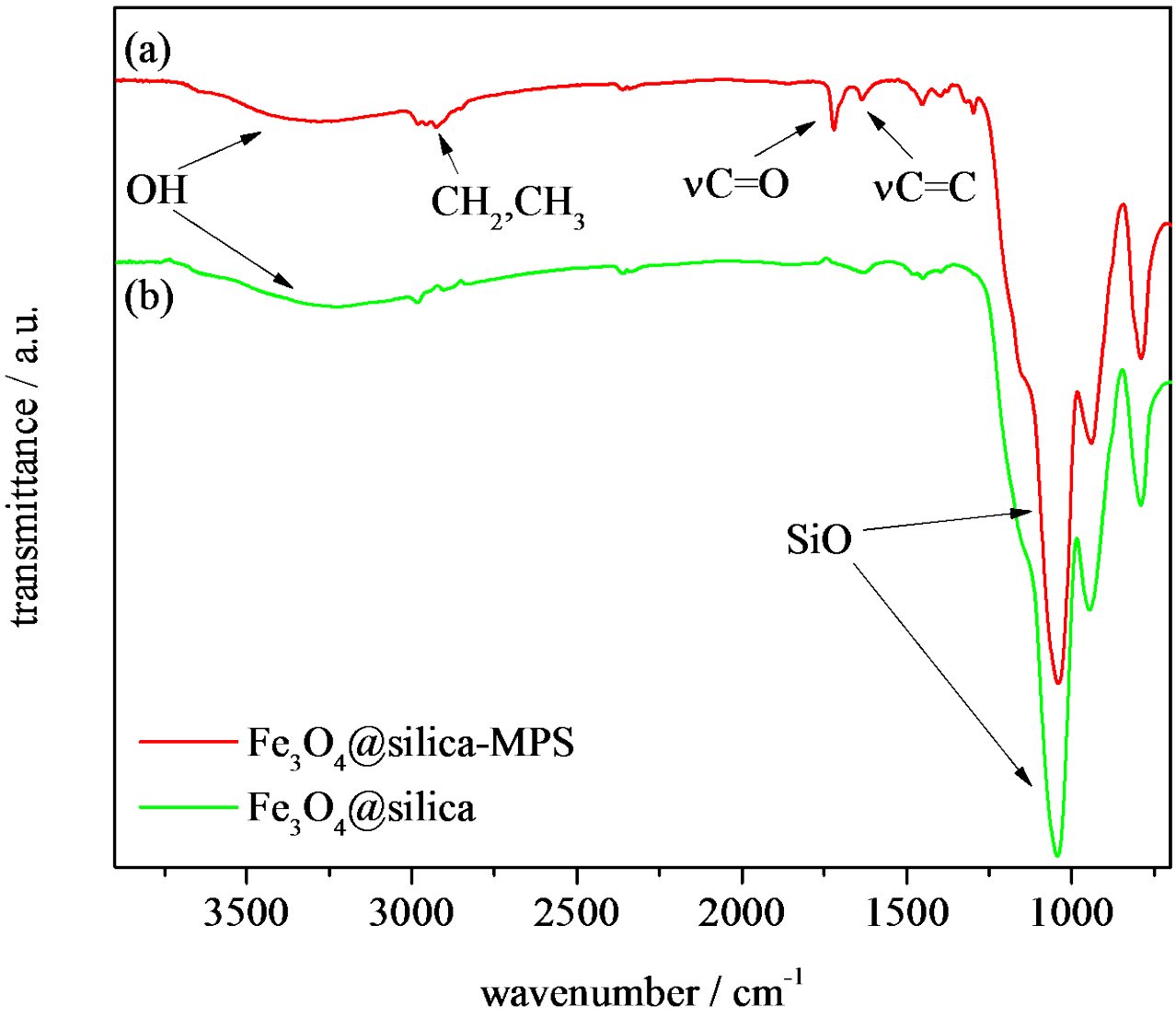

Figure S4. FT-IR spectrum of the non-functionalized (a) and MPS-functionalized (b) Fe_3O_4@silica nanoparticles.

The FTIR spectra of the particles show absorption bands arising from asymmetric vibration of Si-O (1050 cm^{-1}), asymmetric vibration of Si-OH (945 cm^{-1}), and symmetric vibration of Si-O (795 cm^{-1}).[2] The broadband centered between 3300 cm^{-1} and 3500 cm^{-1} is assigned to the fundamental stretching vibrations of different hydroxyl groups, such as those due to adsorbed water.[2] The peaks at 2945 cm^{-1} (CH_3) and 2915 cm^{-1} (CH_2) can be used to identify either the presence of MPS onto the silica surface and unreacted TEOS in the particles.[3] As a matter of fact, these peaks are more evident for MPS-functionalized nanoparticles, supporting the first hypothesis. The presence in

the spectrum of MPS-functionalized core-shell nanoparticles (a) of the two peaks at 1720 cm^{-1} and 1637 cm^{-1} assigned to C=O and C=C stretching,[4] respectively, indicates the goodness of the proposed functionalization procedure.

[1] E.P. Furlani, *Permanent magnet & electromechanical devices: materials, analysis and applications*, Academic press, San Diego, CA, USA 2001.

[2] Y. Ding, X. Chu, X. Hong, P. Zou, Y. Liu, *Appl. Phys. Lett.,* 2012, **100**, 013701.

[3] K.M. Bratlie, H. Lee, K. Komvopoulos, P. Yang, G.A. Somorjai, *Nano Lett.,* 2007, **7**, 3097.

[4] L.-V. Daimay, B.C. Norman, W.G. Fateley, J.G. Grasselli, *The Handbook of Infrared and Raman Characteristic Frequencies of Organic Molecules*, Academic press, London, UK 1991.